NeuroImage: Clinical 19 (2018) 14–21

Contents lists available at ScienceDirect

NeuroImage: Clinical

journal homepage: www.elsevier.com/locate/ynicl

The association of regional white matter lesions with cognition in a community-based cohort of older individuals

Jiyang Jiang[a,*], Matthew Paradise[a], Tao Liu[b], Nicola J. Armstrong[c], Wanlin Zhu[a,d,e], Nicole A. Kochan[a,f], Henry Brodaty[a,g], Perminder S. Sachdev[a,f], Wei Wen[a,f]

[a] Centre for Healthy Brain Ageing, School of Psychiatry, University of New South Wales, Australia
[b] School of Biological Science and Medical Engineering, Beihang University, Beijing, China
[c] Mathematics and Statistics, Murdoch University, Murdoch, WA, Australia
[d] Department of Radiology, Beijing Tiantan Hospital, Capital Medical University, Beijing, China
[e] Tiantan Image Research Center, China National Clinical Research Center for Neurological Diseases, Beijing, China
[f] Neuropsychiatric Institute, Prince of Wales Hospital, Randwick, NSW, Australia
[g] Dementia Centre for Research Collaboration, School of Psychiatry, UNSW Australia, Sydney, NSW, Australia

ARTICLE INFO

Keywords:
White matter lesions
Strategic white matter fiber tracts
Cognitive performance
Neuropsychological assessments
Community-dwelling older individuals

ABSTRACT

Emerging evidence from lesion-symptom mapping (LSM) studies suggested that regional white matter lesions (WML) on strategic white matter (WM) fiber tracts are significantly associated with specific cognitive domains, independent of global WML burden. However, previous LSM investigations were mostly carried out in disease cohorts, with little evidence from community-based older individuals, making findings difficult to generalize. Moreover, most LSM studies applied a threshold to the probabilistic atlas, leading to the loss of information and threshold-dependent findings. Furthermore, it is still unclear whether associations between regional WML and cognition are independent of global grey matter (GM) and WM volumes, which have also been linked to cognition. In the current study, we undertook a region of interest (ROI) LSM study to examine the relationship between regional WML on strategic WM tracts and cognitive performance in a large community-based cohort of older individuals (N = 461; 70–90 years). WML were extracted using a publicly available pipeline, UBO Detector (https://cheba.unsw.edu.au/group/neuroimaging-pipeline). Mapping of WML to the Johns Hopkins University WM atlas was undertaken using an automated TOolbox for Probabilistic MApping of Lesions (TOPMAL), which we introduce here, and is implemented in UBO Detector. The results show that different patterns of brain structural volumes in the ageing brain were associated with different cognitive domains. Regional WML were associated with processing speed, executive function, and global cognition, independent of total GM, WM and WML volumes. Moreover, regional WML explained more variance in executive function, compared to total GM, WM and WML volumes. The current study highlights the importance of studying regional WML in age-related cognitive decline.

1. Introduction

Cerebral small vessel disease (CSVD) is the most common cerebrovascular dysfunction, and one of the leading causes of dementia and strokes in older adults (Pantoni, 2010). As an ischemic biomarker of CSVD, the accumulation of white matter lesions (WML) has been closely associated with cognitive decline (Prins and Scheltens, 2015). In addition, WML have been found to be prominent in both middle aged (Wen et al., 2009) and general ageing (Maniega et al., 2015) populations. However, due to technical limitations and the historical perspective of global effects of cerebral structural degeneration on cognition and neuropathology, the vast majority of studies investigating the relationship of WML with cognition have focused on global WML, disregarding location information (Biesbroek et al., 2017).

With the growing acknowledgement that periventricular (PVWML) and deep (DWML) WML have different albeit overlapping etiologies and risk factors (Sachdev, 2005), and that lobar WML are associated with characteristic cognitive domains (van der Vlies et al., 2013), studies have started to investigate localized WML in relation to cognition and neuropathology. Finer mapping of WML to strategic white matter (WM) fiber tracts, and lacunar infarcts onto subcortical structures, has also been examined in more recent lesion-symptom mapping (LSM)

* Corresponding author at: R1f building, 22-32 King Street, Randwick 2031, NSW, Australia.
E-mail address: jiyang.jiang@unsw.edu.au (J. Jiang).

https://doi.org/10.1016/j.nicl.2018.03.035
Received 20 November 2017; Received in revised form 2 March 2018; Accepted 28 March 2018
Available online 29 March 2018

studies (Biesbroek et al., 2017). In these studies, processing speed and executive function have been commonly associated with CSVD-related lesions on two strategic WM tracts, anterior thalamic radiation (ATR) and forceps minor (Biesbroek et al., 2016; Duering et al., 2011). Additionally, processing speed has also been associated with cingulate cortex, forceps major and corticospinal tract (CST) (Duering et al., 2013; Duering et al., 2011), and executive function has been linked with lesions on superior longitudinal fasciculus (SLF) (Biesbroek et al., 2013). Available studies have also suggested associations of memory with forceps minor and forceps major tracts (Biesbroek et al., 2016; Duering et al., 2011).

Studies investigating the relationships of lesions on different strategic WM tracts with cognitive domains, have been undertaken in several different cohorts, including disease cohorts of individuals diagnosed with cerebral autosomal dominant arteriopathy with subcortical infarcts and leukoencephalopathy (CADASIL), arterial diseases, stroke, and CSVD. Findings from the two community-based studies which examined LSM were inconsistent (Duering et al., 2014; Smith et al., 2011). This makes drawing conclusions from available findings tenuous and needing caution. Moreover, although some studies have taken into account the probability of the WML voxels belonging to each WM tract (Duering et al., 2014; Duering et al., 2013), others have applied a 10%–25% threshold to binarize the probability atlases (Benjamin et al., 2014; Biesbroek et al., 2016; Duering et al., 2011) which ignores the information contained in the probabilities, and may make any conclusions dependent on the choice of threshold. In addition, it is still unknown if the relationships between regional WML and cognition are independent of the association between grey matter (GM) volumes and cognition, given that WML and GM atrophy share similar risk factors and are significantly correlated with each other (Raji et al., 2012; Wen et al., 2006).

In this study, we examined the relationship of WML burden on strategic WM tracts with cognitive domains, including processing speed, executive function, memory, language and visuo-spatial function, as well as diagnostic classifications [mild cognitive impairment (MCI) *vs.* cognitively normal (CN)], in a large community-based cohort of non-demented older adults. WML maps were generated from a fully automated pipeline for WML segmentation, UBO Detector (Wen et al., 2009), we recently made freely available at https://cheba.unsw.edu.au/group/neuroimaging-pipeline. The mapping of WML burden to strategic WM tracts atlas was undertaken by TOPMAL (TOolbox for Probabilistic MApping of Lesions), an extension of UBO Detector which is described in the current paper. We hypothesized that WML burden on strategic WM tracts would not contribute equally to different cognitive domains, and that the association of regional WML with cognition was independent of global structural deficit, including global GM and WM atrophy.

2. Materials and methods

2.1. Study sample

The study sample was drawn from Sydney Memory and Ageing Study (Sydney MAS), a community-based study of non-demented older adults aged 70–90 years at baseline living in Sydney, Australia (Sachdev et al., 2010). Individuals were excluded if they had a previous diagnosis or current evidence of dementia, mental retardation, psychotic disorder including schizophrenia or bipolar disorder, multiple sclerosis, motor neuron disease, developmental disability, or progressive malignancy. 1037 participants were finally included in the baseline of Sydney MAS.

Five hundred and thirty-nine of the 1037 participants received MRI scans. Since insufficient English skill may significantly confound the performance in neuropsychological tests, we further excluded 73 participants with non-English speaking background (i.e. not speaking English in the conversational level since the age of < 10 years). Therefore, 466 participants were included in the current study.

2.2. MRI acquisition

Two hundred and forty of the 466 scans were acquired from a Philips 3 T Intera Quasar scanner (Philips Medical Systems, The Netherlands), whereas the remaining 226 participants were scanned on a Philips 3 T Achieva Quasar Dual scanner. A dummy variable indicating scanner has been used in all statistical analyses to account for any scanner differences. The two scanners were set to the same scanning parameters:

2.2.1. T1-weighted MRI

Repetition time (TR) = 6.39 ms, echo time (TE) = 2.9 ms, flip angle = 8°, matrix size = 256 × 256, FOV (field of view) = 256 × 256 × 190, and slice thickness = 1 mm with no gap in between, yielding 1 × 1 × 1 mm^3 isotropic voxels.

2.2.2. T2-weighted Fluid Attenuated Inversion Recovery (FLAIR) sequence

TR = 10,000 ms, TE = 110 ms, inversion time (TI) = 2800 ms, matrix size = 512 × 512, slice thickness = 3.5 mm without gap, and in plane resolution = 0.488 × 0.488 mm.

2.3. Neuropsychological assessment and diagnostic classification

The component tests of the five cognitive domains, namely processing speed, executive function, memory, visuo-spatial function, and language, in Sydney MAS have been described previously (Sachdev et al., 2010), and summarized in Supplementary Table 1. Raw scores were converted to quasi *z*-scores using the baseline mean and standard deviation (SD) values for a healthy reference group which consists of 723 healthy Sydney MAS participants who were fluent in English before 10 years old and free of dementia, neurological and psychiatric disorders, and central nervous system (CNS) medications at baseline. Domain scores were calculated by averaging *z*-scores of the component tests with the exception of the visuo-spatial domain represented by a single test. A global cognition score was calculated by averaging the domain scores. All domain and global cognition scores were standardised so that the reference group had means and SDs of 0 and 1.

The diagnosis of MCI was made according to international consensus criteria (Petersen, 2004; Winblad et al., 2004): 1) a subjective complaint of decline in memory or other cognitive function; 2) cognitive impairment as shown by performance 1.5 standard deviation (SD) below published normative values; 3) normal or minimally impaired functional activities as determined by informant ratings on the Bayer-ADL scale (Hindmarch et al., 1998); 4) no diagnosis of DSM-IV dementia. CN participants had a performance on all neuropsychological test measures which was above the impairment criterion above. The diagnosis of dementia was made by an expert panel of clinicians according to DSM-IV criteria, using information from a clinical interview, comprehensive neuropsychological test battery, informant-based report of instrumental activities of daily living and neuropsychiatric symptoms, and MRI. Participants with the diagnosis of dementia were excluded. In the 466 participants included in the current study, 293 were classified as CN and 173 were diagnosed with MCI.

2.4. WML segmentation

T1-weighted and FLAIR scans of the 466 participants were processed with UBO Detector (https://cheba.unsw.edu.au/group/neuroimaging-pipeline) for the segmentation of WML regions. The algorithm has been described previously (Wen et al., 2009). Briefly, FLAIR images were registered to T1, and then warped to Diffeomorphic Anatomical Registration Through Exponentiated Lie Algebra (DARTEL) space. After non-brain tissue removal, FMRIB's Automated Segmentation Tool (FAST) was applied to FLAIR data to generate candidate clusters. A supervised learning algorithm, k-nearest neighbours (*k*-NN), was used to determine WML clusters. Default settings with $k = 5$ and

probability threshold of 0.7 were used for the WML segmentation in the current study. Results were manually checked for segmentation quality. Five scans were excluded due to significant scanner artefacts.

2.5. WML mapping to strategic WM tracts using TOPMAL

TOPMAL is a toolbox to map CSVD-related lesions to brain atlases, including John Hopkins University (JHU) WM Tractography Atlas (Hua et al., 2008) and Harvard-Oxford Subcortical Structural Atlas (Desikan et al., 2006). The output can be directly used for region of interest (ROI) LSM analyses (Biesbroek et al., 2017).

TOPMAL was developed as an extension of UBO Detector (https://cheba.unsw.edu.au/group/neuroimaging-pipeline) which is an automated pipeline for WML extraction. It can also be applied to the anatomical mapping of other types of CSVD-related lesions, such as lacunar infarcts, dilated perivascular space, and microbleeds. In the current study, we used TOPMAL to map WML to JHU WM atlas. The WML masks from UBO Detector were in a standard space (DARTEL space) (Ashburner, 2007), which enables further analyses regarding the location of lesions. Flow field map was applied to JHU WM atlas to bring it to DARTEL space, and the resultant atlas was then applied to WML maps derived from UBO Detector. The resultant image contained the regions of WML overlapping with strategic WM tracts on JHU WM atlas.

2.5.1. Lesion loading calculation

In TOPMAL, the lesion loading takes into account the probability of each WML voxel belonging to the WM tract. Each voxel has a series of probabilities, treated here as weights, which represent the likelihood of the voxel belonging to each of the WM tracts. Using these weights, TOPMAL calculates, for each WM tract:

$$absolute\ WML\ loading = \sum_{i=1}^{N_{vox}} WML_i * WMTprob_i$$

where N_{vox} is the number of voxels in the MRI scan; WML_i denotes whether voxel i is WML or non-WML (i.e. 1 or 0); and WMT_prob_i is the probability of voxel i belonging to the WM tract.

$$fractional\ loading = \frac{absolute\ loading}{\sum_{i=1}^{N_{vox}} WMTprob_i} = \frac{\sum_{i=1}^{N_{vox}} WML_i * WMTprob_i}{\sum_{i=1}^{N_{vox}} WMTprob_i}$$

Fractional loading for a WM tract is defined to be the standardised absolute WML loadings, which takes into account the weights of all voxels with respect to the tract. This quantity is useful for within-subject between-tracts comparisons of WML loadings. TOPMAL also returns, for each strategic WM tract, the number of WML voxels for which the probability of belonging to the WM tract is greater than 0 ($N_{WMT \cap WML}$). In addition, TOPMAL also calculates total void loadings to indicate the sum of WML loadings for voxels not belonging to strategic WM tracts in the JHU WM atlas (see Supplementary Text for more details).

2.6. Total GM and WM volumes

The standard FreeSurfer processing pipeline (Fischl et al., 2002) was applied to T1-weighted scans for brain tissue segmentation, and total, cortical and subcortical GM volumes as well as total WM volumes were calculated. The segmentation was manually checked and edited following the procedures described on https://surfer.nmr.mgh.harvard.edu/fswiki/Edits.

2.7. Statistical analyses

The association between WML and cognition was assessed using the absolute WML loadings, as defined above. For total GM and WM volumes as well as cortical and subcortical GM volumes, the effects of intracranial volume (ICV) and scanner were removed by regression, with the residuals being used in the following analyses. For total WML, PVWML and DWML volumes calculated in DARTEL space, adjustment was made only for scanner, but not ICV. All results were reported in raw *p*-values. Those survived Bonferroni correction for multiple tests for the 20 WM tracts were also marked and reported. Mathematical equations of the applied statistical models have been included in the Supplementary Text.

Regression analyses were carried out to examine the relationships of global structural measures (total, cortical and subcortical GM, total WM, total WML, PVWML and DWML volumes) and WML loadings on strategic WM tracts with cognitive domain scores (processing speed, language, executive function, visuo-spatial function, and memory scores, as well as global cognition score). In each instance, the cognitive domain score was the dependent variable while a global volume or regional WML loading measure (adjusted for scanner and ICV if appropriate) was the independent variable. Additionally, demographic variables were taken into account by including age, sex and years of education as covariates. Association is tested using the standard Wald test for whether the coefficient of the neuroimaging index is equal to 0 (i.e. no association) or not. For those indices found to be significantly associated with cognition, hierarchical regression analyses were then carried out, to examine the additive effect of each of these neuroimaging indices on cognition in addition to demographic factors. Changes in R^2 and the corresponding *p*-values are reported for comparison.

Similarly, to investigate differences between CN and MCI, logistic regression models were used. In this case, the dependent variable was CN or MCI (coded as 0 and 1 respectively). The independent variables were again each of the neuroimaging measures and demographic variables. Significant of differences was determined using the Wald test for whether the coefficient of the neuroimaging index is equal to 0 or not in the regression model.

Fractional WML loadings were used for between-tracts comparisons. Specifically, we used a one-way repeated measures ANCOVA to determine if the mean level of fractional WML loadings differed between the 20 strategic WM tracts in the JHU WM atlas, adjusting for demographic factors (age, sex and education level) and scanner. Specifically, we tested the null hypothesis that $\mu_1 = \mu_2 = \ldots = \mu_{20}$, where μ_i is the mean fractional WML loadings for the WM tract *i*, against the alternative that they are not all equal. After testing for overall differences, post-hoc comparisons between each of the pairs of WM tracts were then conducted, using the Bonferroni correction for multiple comparisons.

3. Results

3.1. Characteristics of the study sample

The characteristics of the study sample are summarized in Table 1. The age range was 70–90 years, and the duration of education ranged from 3 to 24 years. The output from TOPMAL for Sydney MAS has been summarized in Supplementary Table 2. Total void loadings were, on

Table 1
Characteristics of Sydney MAS participants.

N	461[a]
Age (years)	78.26 ± 4.65
Sex (%Female)	56.1
Years of education (years)	11.79 ± 3.60
Whole brain WML volume (mm^3)	19,400.83 ± 19,057.11
NART predicted IQ	108.04 ± 9.83
MMSE[b]	28.61 ± 1.25

[a] Five hundred and thirty-nine participants were scanned at the baseline of Sydney MAS. Of the 539 participants, 73 participants with non-English speaking background were excluded from the current study. Five scans were further excluded due to significant scanner artefact.

[b] MMSE scores were adjusted for age and years of education. NART – national adult reading test; MMSE – mini-mental state examination.

Table 2
The associations of global measures with cognition.

	Processing speed		Language		Executive function		Visuo-spatial ability		Memory		Global cognition		CN vs. MCI[c]		
	β	*p*	β	*p*	β	*p*	β	*p*	β	*p*	β	*p*	B	SE	*p*
Total GM [a]	0.205	< 0.001[d]	0.170	0.001[d]	0.113	0.024	0.278	< 0.001[d]	0.074	0.120	0.236	< 0.001[d]	−1.6E-5	3.0E-6	< 0.001[d]
Cortical GM [a]	0.167	0.001[d]	0.139	0.005[d]	0.096	0.053	0.281	< 0.001[d]	0.060	0.200	0.209	< 0.001[d]	−1.9E-5	4.0E-6	< 0.001[d]
Subcortical GM [a]	0.130	0.005[d]	0.122	0.009	0.060	0.198	0.154	0.001[d]	0.051	0.244	0.154	< 0.001[d]	−7.5E-5	2.2E-5	0.001[d]
Total WM [a]	0.248	< 0.001[d]	0.067	0.178	0.113	0.021	0.179	< 0.001[d]	−0.024	0.603	0.176	< 0.001[d]	−5.0E-6	3.0E-6	0.067
Total WML [b]	−0.172	< 0.001[d]	−0.078	0.095	−0.187	< 0.001[d]	−0.080	0.073	−0.011	0.797	−0.143	0.001[d]	8.0E-6	6.0E-6	0.132
PVWML [b]	−0.161	0.001[d]	−0.077	0.102	−0.189	< 0.001[d]	−0.087	0.055	−0.011	0.800	−0.141	0.001[d]	1.7E-5	1.2E-5	0.147
DWML [b]	−0.152	0.001[d]	−0.066	0.154	−0.157	0.001[d]	−0.060	0.175	−0.011	0.804	−0.122	0.004[d]	1.2E-5	9.0E-6	0.186

GM – grey matter; WM – white matter; WML – white matter lesions; PVWML – periventricular WML; DWML – deep WML.
[a] Residuals after regressing out the effects of scanner and intracranial volume (ICV) were used.
[b] Residuals after regressing out the effects of scanner were used as WML volumes generated by UBO Detector has accounted for ICV.
[c] 290 CN and 171 MCI participants.
[d] Significant after Bonferroni correction.

Table 3
The associations of WML loadings on strategic white matter fiber tracts with cognitive domains.

Strategic white matter tracts	Processing speed		Language		Executive function		Visuo-spatial		Memory		Global cognition		CN vs. MCI[a]		
	β	*p*	β	*p*	β	*p*	β	*p*	β	*p*	β	*p*	B	SE	*p*
lATR	−0.188	< 0.001[b]	−0.082	0.081	−0.198	< 0.001[b]	−0.091	0.045	−0.032	0.474	−0.159	< 0.001[b]	0.002	0.001	0.094
rATR	−0.172	< 0.001[b]	−0.093	0.051	−0.174	< 0.001[b]	−0.097	0.034	−0.004	0.932	−0.147	0.001[b]	0.002	0.001	0.132
lCST	−0.212	< 0.001[b]	−0.098	0.036	−0.220	< 0.001[b]	−0.108	0.016	−0.029	0.513	−0.182	< 0.001[b]	0.006	0.003	0.042
rCST	−0.201	< 0.001[b]	−0.107	0.021	−0.198	< 0.001[b]	−0.124	0.005	−0.049	0.276	−0.184	< 0.001[b]	0.007	0.003	0.030
lCCG	−0.109	0.017	−0.013	0.783	−0.128	0.005	−0.031	0.487	−0.023	0.608	−0.083	0.054	0.008	0.007	0.290
rCCG	−0.135	0.003	−0.045	0.334	−0.116	0.011	−0.099	0.025	0.005	0.907	−0.108	0.011	0.020	0.018	0.285
lCH	−0.057	0.217	−0.037	0.426	−0.019	0.677	−0.089	0.044	−0.046	0.298	−0.062	0.149	−0.001	0.069	0.987
rCH	−0.155	0.001[b]	−0.094	0.044	−0.129	0.006	−0.118	0.008	−0.085	0.058	−0.157	< 0.001[b]	0.089	0.043	0.036
FMa	−0.105	0.025	−0.036	0.441	−0.077	0.101	−0.122	0.007	0.007	0.882	−0.092	0.036	0.001	0.001	0.443
FMi	−0.157	0.001[b]	−0.071	0.128	−0.163	< 0.001[b]	−0.067	0.138	0.003	0.951	−0.126	0.004	0.001	0.001	0.174
lIFOF	−0.121	0.009	−0.042	0.370	−0.147	0.002[b]	−0.085	0.057	−0.002	0.960	−0.110	0.011	0.001	0.001	0.506
rIFOF	−0.153	0.001[b]	−0.049	0.296	−0.125	0.007	−0.121	0.007	0.016	0.718	−0.121	0.005	0.001	0.001	0.328
lILF	−0.084	0.071	−0.008	0.868	−0.085	0.067	−0.076	0.088	0.024	0.592	−0.064	0.141	−0.001	0.002	0.803
rILF	−0.122	0.008	−0.030	0.511	−0.099	0.032	−0.112	0.012	0.009	0.835	−0.098	0.023	0.002	0.002	0.533
lSLF	−0.164	< 0.001[b]	−0.060	0.193	−0.175	< 0.001[b]	−0.085	0.057	−0.028	0.523	−0.138	0.001[b]	0.001	0.001	0.185
rSLF	−0.197	< 0.001[b]	−0.082	0.078	−0.205	< 0.001[b]	−0.078	0.080	−0.028	0.534	−0.157	< 0.001[b]	0.002	0.001	0.033
lUF	−0.132	0.004	−0.069	0.138	−0.165	< 0.001[b]	−0.059	0.183	−0.028	0.535	−0.125	0.004	0.006	0.004	0.187
rUF	−0.144	0.002[b]	−0.087	0.065	−0.115	0.015	−0.100	0.027	−0.024	0.589	−0.118	0.007	0.017	0.011	0.126
lSLFT	−0.163	< 0.001[b]	−0.059	0.201	−0.174	< 0.001[b]	−0.090	0.042	−0.025	0.571	−0.139	0.001[b]	0.003	0.002	0.172
rSLFT	−0.195	< 0.001[b]	−0.079	0.089	−0.196	< 0.001[b]	−0.068	0.128	−0.021	0.635	−0.148	0.001[b]	0.006	0.003	0.026

lATR – left anterior thalamic radiation; rATR – right anterior thalamic radiation; lCST - left corticospinal tract; rCST - right corticospinal tract; lCCG – left cingulum (cingulate gyrus); rCCG – right cingulum (cingulate gyrus); lCH – left cingulum (hippocampus); rCH – right cingulum (hippocampus); FMa - forceps major; FMi - forceps minor; lIFOF – left inferior fronto-occipital fasciculus; rIFOF – right inferior fronto-occipital fasciculus; lILF – left inferior longitudinal fasciculus; rILF – right inferior longitudinal fasciculus; lSLF – left superior longitudinal fasciculus; rSLF – right superior longitudinal fasciculus; lUF – left uncinate fasciculus; rUF – right uncinate fasciculus; lSLFT – left superior longitudinal fasciculus (temporal part); rSLFT – right superior longitudinal fasciculus (temporal part).
[a] 290 CN and 171 MCI participants.
[b] Significant after Bonferroni correction.

average, over five times greater than the sum of WML loadings on strategic WM tracts (range 2.08–26.99).

3.2. The associations of global measures with cognition

All tested global structural measures were associated with processing speed and global cognition after Bonferroni correction (Table 2). Higher total GM volume, especially in cortical regions, was associated with better performance in language, whereas more WML, including both PVWML and DWML, was linked to poorer executive function. Higher total GM volume, including both cortical and subcortical GM regions, and total WM volume were associated with better visuo-spatial function, after Bonferroni correction. CN participants had higher volumes in GM, including both cortical and subcortical regions, but not in WM or WML, compared to MCI participants. Memory was not associated with any of the examined global structural measures.

3.3. The associations of WML loadings on strategic WM tracts with cognition

The relationships between WML loadings on strategic WM tracts and cognitive domains are summarized in Table 3. Processing speed and executive function shared mostly common strategic WM tracts with higher WML loadings being associated with poorer performance. These common tracts include forceps minor, as well as bilateral ATR, CST and SLF including the temporal part. Processing speed was also associated with the hippocampal part of cingulum on the right hemisphere (right CH), right inferior fronto-occipital fasciculus (IFOF), and right uncinate fasciculus (UF), whereas executive function was additionally associated with IFOF and UF on the left hemisphere. Higher WML loadings on bilateral ATR, CST and SLF (including temporal part), as well as right CH were also associated with worse global cognition. Language, visuo-spatial function, memory, and CN/MCI classification were not

Table 4
The associations between regional WML loadings and cognitive performance after adjusting for global volumetric measures.

		Additional covariate													
		Total GM		Cortical GM		Subcortical GM		Total WM		Total WML		PVWML		DWML	
		β	*p*	β	*p*	β	*p*	β	*p*	β	*p*	β	*p*	β	*p*
Processing speed	lATR	**−0.167**	**< 0.001***	**−0.170**	**< 0.001***	**−0.201**	**< 0.001***	**−0.147**	**0.002***	−0.153	0.097	**−0.188**	**0.033**	**−0.161**	**0.017**
	rATR	**−0.142**	**0.003***	**−0.147**	**0.002***	**−0.187**	**< 0.001***	**−0.130**	**0.006**	−0.086	0.272	−0.118	0.169	**−0.121**	**0.049**
	lCST	**−0.185**	**< 0.001***	**−0.190**	**< 0.001***	**−0.210**	**< 0.001***	**−0.166**	**< 0.001***	**−0.202**	**0.008**	**−0.218**	**0.003***	**−0.199**	**0.002***
	rCST	**−0.176**	**< 0.001***	**−0.180**	**< 0.001***	**−0.205**	**< 0.001***	**−0.163**	**< 0.001***	**−0.196**	**0.022**	**−0.190**	**0.007**	**−0.204**	**0.005**
	rCH	**−0.126**	**0.007**	**−0.130**	**0.005**	**−0.157**	**0.001***	**−0.118**	**0.010**	−0.071	0.252	−0.082	0.229	−0.103	0.054
	FMi	**−0.138**	**0.003***	**−0.141**	**0.002***	**−0.166**	**< 0.001***	**−0.121**	**0.008**	−0.068	0.307	−0.083	0.244	−0.102	0.068
	rIFOF	**−0.123**	**0.008**	**−0.128**	**0.007**	**−0.155**	**0.001***	**−0.114**	**0.013**	0.015	0.887	−0.056	0.558	−0.084	0.252
	lSLF	**−0.135**	**0.003***	**−0.140**	**0.003***	**−0.159**	**< 0.001***	**−0.129**	**0.005**	−0.061	0.535	−0.105	0.098	−0.136	0.171
	rSLF	**−0.166**	**< 0.001***	**−0.172**	**< 0.001***	**−0.194**	**< 0.001***	**−0.160**	**< 0.001***	**−0.187**	**0.031**	**−0.169**	**0.008**	**−0.226**	**0.006**
	rUF	**−0.115**	**0.015**	**−0.119**	**0.012**	**−0.154**	**0.001**	**−0.095**	**0.044**	−0.046	0.474	−0.061	0.349	−0.082	0.146
	lSLFT	**−0.133**	**0.004***	**−0.138**	**0.003***	**−0.158**	**0.001***	**−0.130**	**0.004***	−0.062	0.493	−0.103	0.111	−0.121	0.158
	rSLFT	**−0.162**	**< 0.001***	**−0.169**	**< 0.001***	**−0.190**	**< 0.001***	**−0.156**	**0.001***	**−0.168**	**0.036**	**−0.165**	**0.010**	**−0.194**	**0.008**
Executive function	lATR	**−0.189**	**< 0.001***	**−0.190**	**< 0.001***	**−0.204**	**< 0.001***	**−0.185**	**< 0.001***	−0.137	0.135	−0.136	0.122	0.082	0.685
	rATR	**−0.162**	**0.001***	**−0.164**	**0.001***	**−0.182**	**< 0.001***	**−0.159**	**0.001***	−0.057	0.471	−0.046	0.593	−0.119	0.052
	lCST	**−0.210**	**< 0.001***	**−0.212**	**< 0.001***	**−0.219**	**< 0.001***	**−0.207**	**< 0.001***	**−0.192**	**0.011**	**−0.186**	**0.010**	**−0.209**	**0.001***
	rCST	**−0.188**	**< 0.001***	**−0.190**	**< 0.001***	**−0.200**	**< 0.001***	**−0.186**	**< 0.001***	−0.141	0.100	−0.133	0.058	**−0.189**	**0.009**
	FMi	**−0.154**	**0.001***	**−0.155**	**0.001***	**−0.168**	**< 0.001***	**−0.150**	**0.001***	−0.057	0.387	−0.047	0.507	−0.107	0.056
	lIFOF	**−0.138**	**0.003***	**−0.139**	**0.003***	**−0.149**	**0.001***	**−0.135**	**0.004***	0.122	0.254	0.020	0.803	−0.052	0.514
	lSLF	**−0.163**	**< 0.001***	**−0.165**	**< 0.001***	**−0.173**	**< 0.001***	**−0.162**	**< 0.001***	−0.049	0.617	−0.089	0.155	−0.171	0.090
	rSLF	**−0.194**	**< 0.001***	**−0.197**	**< 0.001***	**−0.204**	**< 0.001***	**−0.193**	**< 0.001***	**−0.172**	**0.048**	**−0.148**	**0.020**	**−0.245**	**0.003***
	lUF	**−0.155**	**0.001***	**−0.157**	**0.001***	**−0.168**	**< 0.001***	**−0.152**	**0.001***	−0.068	0.285	−0.081	0.157	−0.108	0.073
	lSLFT	**−0.162**	**0.001***	**−0.165**	**< 0.001***	**−0.172**	**< 0.001***	**−0.162**	**< 0.001***	−0.054	0.552	−0.087	0.175	−0.149	0.087
	rSLFT	**−0.184**	**< 0.001***	**−0.187**	**< 0.001***	**−0.194**	**< 0.001***	**−0.183**	**< 0.001***	−0.133	0.100	**−0.129**	**0.044**	**−0.189**	**0.010**
Global cognition	lATR	**−0.131**	**0.002***	**−0.133**	**0.002***	**−0.171**	**< 0.001***	**−0.129**	**0.003***	−0.132	0.124	−0.142	0.087	**−0.145**	**0.022**
	rATR	**−0.110**	**0.012**	**−0.112**	**0.012**	**−0.163**	**< 0.001***	**−0.117**	**0.008**	−0.082	0.266	−0.092	0.255	−0.112	0.051
	lCST	**−0.146**	**0.001***	**−0.149**	**0.001***	**−0.179**	**< 0.001***	**−0.150**	**0.001***	**−0.185**	**0.010**	**−0.183**	**0.007**	**−0.184**	**0.002***
	rCST	**−0.151**	**< 0.001***	**−0.154**	**< 0.001***	**−0.187**	**< 0.001***	**−0.157**	**< 0.001***	**−0.220**	**0.006**	**−0.185**	**0.005***	**−0.219**	**0.001***
	rCH	**−0.122**	**0.005***	**−0.123**	**0.005***	**−0.159**	**< 0.001***	**−0.132**	**0.002***	−0.110	0.060	−0.118	0.065	**−0.127**	**0.012**
	lSLF	**−0.103**	**0.016**	**−0.105**	**0.014**	**−0.132**	**0.002***	**−0.114**	**0.008**	−0.058	0.507	−0.082	0.165	−0.134	0.132
	rSLF	**−0.119**	**0.006**	**−0.122**	**0.005***	**−0.153**	**< 0.001***	**−0.131**	**0.002***	−0.126	0.113	**−0.117**	**0.050**	**−0.172**	**0.022**
	lSLFT	**−0.102**	**0.017**	**−0.105**	**0.015**	**−0.133**	**0.002***	**−0.116**	**0.007**	−0.065	0.433	−0.083	0.166	−0.123	0.115
	rSLFT	**−0.107**	**0.013**	**−0.110**	**0.011**	**−0.143**	**0.001***	**−0.121**	**0.005***	−0.096	0.195	−0.101	0.092	**−0.133**	**0.048**

lATR – left anterior thalamic radiation; rATR – right anterior thalamic radiation; lCST - left corticospinal tract; rCST - right corticospinal tract; rCH – right cingulum (hippocampus); FMi - forceps minor; lIFOF – left inferior fronto-occipital fasciculus; rIFOF – right inferior fronto-occipital fasciculus; lSLF – left superior longitudinal fasciculus; rSLF – right superior longitudinal fasciculus; lUF – left uncinate fasciculus; rUF – right uncinate fasciculus; lSLFT – left superior longitudinal fasciculus (temporal part); rSLFT – right superior longitudinal fasciculus (temporal part). The β and *p*-values of associations significant at the level of $p \leq 0.05$ were shown in bold. Those remained significant after Bonferroni correction were marked with "*".

associated with WML loadings on any of the examined strategic WM tracts after Bonferroni correction.

Accounting for total WML volumes in additional to demographic factors attenuated some associations between regional WML and cognitive domains, but the ones of WML loadings on bilateral CST and right SLF (including temporal part) with processing speed, left CST and right SLF with executive function, as well as bilateral CST with global cognition, were still significant at the level of $p < 0.05$ (Table 4). All associations of WML loadings on strategic WM tracts with cognition survived further adjustment for total, cortical and subcortical GM volumes as well as total WM volume (all $p < 0.05$), suggesting that the associations were independent of GM and WM atrophy.

3.4. Different contribution of regional WML and global measures to cognition

For the cognitive domains that were significantly associated with both regional WML loadings and global structural measures, hierarchical regression analyses were undertaken to test how much variance in these cognitive domain scores was explained by regional WML loadings and global measures (Table 5). Total WM volumes explained the highest proportion (5.2%) of variance in processing speed scores among all the regional and global measures. This was followed by the 4.3% of variance explained by left CST and 3.9% by right CST. Executive function was only associated with WML measures, and regional WML loadings explained more variance in executive function than global WML volumes. Specifically, WML loadings on left CST accounted for the most variance (4.6%) in executive function scores, followed by right SLF (4.1%). For global cognition, 4.5% of the variance were accounted for by total GM volume, with more contribution from cortical (3.6%) than subcortical (2.3%) region. Total GM volumes (6.3%), especially cortical GM volumes (6.5%, subcortical 2.3%), accounted for more variance in visuo-spatial function than total WM (2.7%).

3.5. Between-tracts comparison of WML fractional loadings

Forceps major showed the greatest fractional WML loadings among the 20 strategic WM tracts, whereas right cingulum (cingulate gyrus) had the least fractional loadings (Fig. 1). Bonferroni *p*-values of the pair-wise comparisons of WML fractional loadings among the 20 strategic WM tracts are shown in Supplementary Table 3.

4. Discussion

In a community-based cohort of 461 older individuals, we examined the associations of WML loadings on strategic WM tracts with cognitive domains and diagnostic classifications (MCI *vs.* CN), and compared them with the relationships of total WML, GM and WM volumes with cognition. The findings suggested that regional WML were independently associated with poorer performance in processing speed and executive function as well as worse global cognition. Different patterns of brain structural measures corresponded with performance in

Table 5
Hierarchical regression analyses for the comparison of the additive effects between regional and global measures to cognition.

	Cognition = demographics + regional/global measure															
	Regional WML			Total GM		Cortical GM		Subcortical GM		Total WM		Total WML		PVWML		DWML	
	WMT	ΔR^2	*p*	ΔR^2	*p*	ΔR^2	*p*	ΔR^2	*p*	ΔR^2	*p*	ΔR^2	*p*	ΔR^2	*p*	ΔR^2	*p*
Processing speed	lATR	0.034	< 0.001	0.034	< 0.001	0.023	0.001	0.016	0.005	**0.052**	**< 0.001**	0.028	< 0.001	0.024	0.001	0.023	0.001
	rATR	0.027	< 0.001														
	lCST	0.043	< 0.001														
	rCST	0.039	< 0.001														
	rCH	0.023	0.001														
	FMi	0.023	0.001														
	rIFOF	0.022	0.001														
	lSLF	0.026	< 0.001														
	rSLF	0.038	< 0.001														
	rUF	0.019	0.002														
	lSLFT	0.026	< 0.001														
	rSLFT	0.037	< 0.001														
Executive function	lATR	0.037	< 0.001	NS	NS	NS	NS	NS	NS	NS	NS	0.034	< 0.001	0.034	< 0.001	0.024	0.001
	rATR	0.028	< 0.001														
	lCST	**0.046**	**< 0.001**														
	rCST	0.038	< 0.001														
	FMi	0.025	< 0.001														
	lIFOF	0.021	0.002														
	lSLF	0.030	< 0.001														
	rSLF	0.041	< 0.001														
	lUF	0.026	< 0.001														
	lSLFT	0.030	< 0.001														
	rSLFT	0.037	< 0.001														
Global cognition	lATR	0.024	< 0.001	**0.045**	**< 0.001**	0.036	< 0.001	0.023	< 0.001	0.026	< 0.001	0.020	0.001	0.019	0.001	0.015	0.004
	rATR	0.020	0.001														
	lCST	0.032	< 0.001														
	rCST	0.033	< 0.001														
	rCH	0.024	< 0.001														
	lSLF	0.019	0.001														
	rSLF	0.024	< 0.001														
	lSLFT	0.019	0.001														
	rSLFT	0.021	0.001														

lATR – left anterior thalamic radiation; rATR – right anterior thalamic radiation; lCST - left corticospinal tract; rCST - right corticospinal tract; lCCG – left cingulum (cingulate gyrus); rCCG – right cingulum (cingulate gyrus); lCH – left cingulum (hippocampus); rCH – right cingulum (hippocampus); FMa - forceps major; FMi - forceps minor; lIFOF – left inferior fronto-occipital fasciculus; rIFOF – right inferior fronto-occipital fasciculus; lILF – left inferior longitudinal fasciculus; rILF – right inferior longitudinal fasciculus; lSLF – left superior longitudinal fasciculus; rSLF – right superior longitudinal fasciculus; lUF – left uncinate fasciculus; rUF – right uncinate fasciculus; lSLFT – left superior longitudinal fasciculus (temporal part); rSLFT – right superior longitudinal fasciculus (temporal part). NS – These associations between global volumetric measures and cognition were not statistical significant after Bonferroni correction (refer to Table 2). The ΔR^2 and corresponding *p*-values for the associations accounting for the most variances in cognition scores were shown in bold.

different cognitive domains in ageing population.

Regarding the associations between regional WML loadings on strategic WM tracts and cognition, the current findings suggest that processing speed and executive function share similar WML distribution patterns, including significant associations with WML loadings on forceps minor, as well as bilateral ATR, CST and SLF (including temporal regions) after Bonferroni correction. Processing speed was also associated with WML loadings on CH, IFOF and UF on the right hemisphere, whereas executive function was additionally associated with IFOF and UF on the left hemisphere. Greater WML on bilateral ATR, CST and SLF including temporal regions, as well as right CH was also associated with poorer global cognition. All the associations between regional WML and cognition were independent of global GM and WM volumes. The relationships of processing speed with bilateral CST and right SLF including temporal part, executive function with left CST and right SLF, as well as global cognition with bilateral CST, were also independent of total WML volumes.

These findings suggest that in community-dwelling older individuals, the distribution of WML associated with processing speed and executive function was similar to that found in disease cohorts (Biesbroek et al., 2017), by showing the associations of ATR and forceps minor with processing speed, and ATR, forceps minor and SLF with executive function. The current study highlights additional involvement of bilateral CST and SLF, as well as CH, IFOF and UF on the right hemisphere in age-related decline in processing speed, as well as bilateral CST, and left UF and IFOF in executive function decline. CST is a major tract critical for sensorimotor function, and responsible for sending movement information from motor, somatosensory and parietal cortices to spinal cord. A longitudinal study of population-based older individuals using diffusion tensor imaging (DTI) showed decreased WM microstructural integrity was associated with worse performance in perceptual speed (Lovden et al., 2014), which was supported by a few cross-sectional investigations, such as (Madden et al., 2012). As a primary motor pathway, CST is also crucial for executive function. SLF is an association fiber tract connecting frontal, occipital, parietal and temporal lobes. Studies have suggested the association of SLF with processing speed (Turken et al., 2008). UF is another long association tract connecting limbic system to orbitofrontal cortex. IFOF connects frontal lobe with occipital and temporal lobes. Both UF and IFOF are crucial association tracts for the ventral intra-hemispheric transfer of information between frontal and occipital, temporal and parietal cortices (Hau et al., 2016). Deficit of WM microstructural integrity on left UF has been associated with worse executive function in individuals with temporal lobe epilepsy (Diao et al., 2015). However, the relationship in an ageing population has not been previously reported. The current finding suggested that processing speed tended to be more associated with the ventral connection between frontal lobe and the rest of the cortices on the right hemisphere, whereas executive

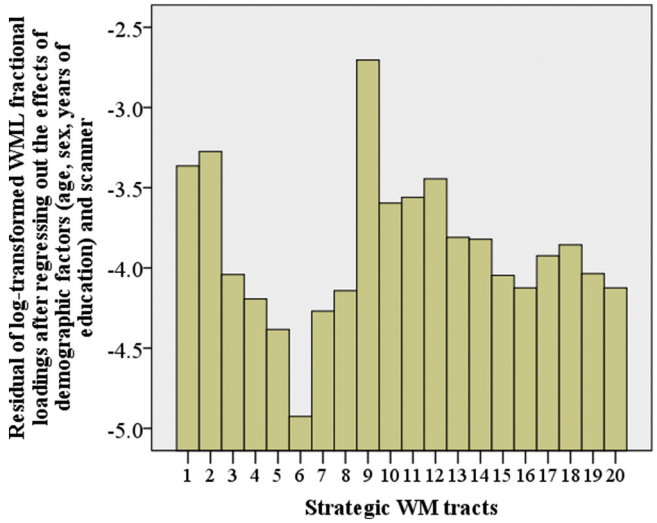

Fig. 1. Comparison of WML fractional (standardised) loadings among the 20 strategic WM tracts. 1 – left anterior thalamic radiation; 2 – right anterior thalamic radiation; 3 – left corticospinal tract; 4 – right corticospinal tract; 5 – left cingulum (cingulate gyrus); 6 – right cingulum (cingulate gyrus); 7 – left cingulum (hippocampus); 8 – right cingulum (hippocampus); 9 – forceps major; 10 – forceps minor; 11 – left inferior fronto-occipital fasciculus; 12 – right inferior fronto-occipital fasciculus; 13 – left inferior longitudinal fasciculus; 14 – right inferior longitudinal fasciculus; 15 – left superior longitudinal fasciculus; 16 – right superior longitudinal fasciculus; 17 – left uncinate fasciculus; 18 – right uncinate fasciculus; 19 – left superior longitudinal fasciculus (temporal part); 20 – right superior longitudinal fasciculus (temporal part).

function was more linked to the connection on the left. However, the hemispheric differences were not statistically significant ($p > 0.05$).

The current study showed that processing speed was linked to all examined measures, including GM, WM and WML volumes, with total WM volumes accounting for the most variance in processing speed scores. Language domain and CN/MCI classification were only associated with GM volume, with greater impact of cortical GM on language function, and higher volumes in both cortical and subcortical GM regions in CN compared to MCI. Both GM and WM volumes, but not WML volumes, were associated with visuo-spatial function, whereas executive function was only associated with WML, but not GM or WM, volumes. Global cognition was associated with all examined global volumetric measures. Total GM volumes, especially cortical GM volumes, explained more variance in visuo-spatial function than total WM volumes. Total GM volumes also accounted for more variance in global cognition. WML loadings on strategic WM tracts, especially bilateral CST as well as left ATR and right SLF including the temporal part, explained more variance in executive function than global WML volumes. In summary, the loss of WM had the most contribution to processing speed, whereas GM atrophy was more associated with performance in language, visuo-spatial, and global cognition, as well as CN/MCI classification. Individuals with greater WML, especially regional WML on bilateral CST, left ATR and right SLF (including temporal part), showed poorer performance in executive function. Since the changes in different brain structural indices are not simultaneous in ageing (Jiang et al., 2014), the distinct associations of age-related cerebral structural degeneration with cognitive domains may underlie asynchronous decline in cognitive domains during ageing (Park and Reuter-Lorenz, 2009), which needs longitudinal studies to confirm.

We also found significantly unequal distribution of WML loadings across strategic WM tracts after taking into account of the size of each tract, with the most WML burden accumulations on forceps major and the least on right cingulum (cingulate gyrus region). Tract-specific WM degeneration in age population has been reported before using DTI data (de Groot et al., 2015), although the distribution is not fully consistent with the current finding. The accumulation of WML on forceps major may indicate the age-related deficit of the splenium of corpus callosum (Pekala et al., 2003). The cingulum is critical for cognitive health in ageing (Metzler-Baddeley et al., 2012). The intactness of cingulum region may be due to the fact that the community-based participants used in the current study were generally experiencing relatively healthy ageing. In addition, the current finding indicated that the previously observed age-related decrease in the volume of cingulum (Mann et al., 2011) may not be of ischemic origin.

The current study did not replicate the results from the only community-based study examining the association of regional WML with memory (Smith et al., 2011). The major differences in the study design of the two studies may contribute to the inconsistency of the conclusion. Smith et al.'s study was carried out on the voxel basis, whereas the current study is a ROI-based investigation. We grouped WML loadings according to strategic WM tracts as our aim was to investigate whether WML accumulations on these tracts were associated with cognition, while in Smith et al.'s study, the voxel-wise analysis was carried out without a specific hypothesis on WM tracts and therefore was not mapped to any WM tractography atlases. The findings from Smith et al.'s voxel-wise analysis were summarized by lobar segmentations, and therefore may not be directly comparable to the current findings.

On average, total void loadings were over five times greater than total WML loadings on strategic WM tracts, suggesting that available JHU WM atlas was not sufficient to conduct a comprehensive LSM study. One of the reasons may be the lack of short WM tracts in the atlas, and this may also partially contribute to the current findings of WML on long tracts being associated with age-related cognitive decline. With the increased accessibility of state-of-the-art MRI techniques, especially ultra-high field, multi-shell and multi-slab DTI with high resolution (Wu et al., 2016), more detailed WM tractography becomes possible (Azadbakht et al., 2015). This will undoubtedly lead to more accurate and comprehensive, and therefore more clinically meaningful lesion mapping.

Another limitation of the current study is that there is an overlap between the component tests of processing speed and executive function. Trail Making Test A used to assess processing speed is highly correlated with Trail Making Test B used for executive function. In addition, component tests of processing speed and executive function domains are timed. These factors may partially explain the overlap of current findings for processing speed and executive function.

In conclusion, we found different patterns of brain structural volumes were associated with different cognitive domains in a community-dwelling sample of older individuals. In addition, we identified independent associations of regional WML on strategic WM tracts with cognitive performance, especially in processing speed and executive function domains. The findings emphasize the association of regional WM deficit with cognitive decline, and the importance of studying the distribution of structural lesions in ageing and neuropathology.

Acknowledgments

The current work was supported by John Holden Family Foundation. We also thank all Sydney MAS participants and the research team.

Appendix A. Supplementary data

Supplementary data to this article can be found online at https://doi.org/10.1016/j.nicl.2018.03.035.

References

Ashburner, J., 2007. A fast diffeomorphic image registration algorithm. NeuroImage 38, 95–113.

Azadbakht, H., Parkes, L.M., Haroon, H.A., Augath, M., Logothetis, N.K., de Crespigny, A.,

D'Arceuil, H.E., Parker, G.J., 2015. Validation of high-resolution tractography against in vivo tracing in the macaque visual cortex. Cereb. Cortex 25, 4299–4309.
Benjamin, P., Lawrence, A.J., Lambert, C., Patel, B., Chung, A.W., MacKinnon, A.D., Morris, R.G., Barrick, T.R., Markus, H.S., 2014. Strategic lacunes and their relationship to cognitive impairment in cerebral small vessel disease. NeuroImage 4, 828–837 Clinical.
Biesbroek, J.M., Kuijf, H.J., van der Graaf, Y., Vincken, K.L., Postma, A., Mali, W.P.T.M., Biessels, G.J., Geerlings, M.I., Grp, S.S., 2013. Association between subcortical vascular lesion location and cognition: a voxel-based and tract-based lesion-symptom mapping study. The SMART-MR study. PLoS One 8.
Biesbroek, J.M., Weaver, N.A., Hilal, S., Kuijf, H.J., Ikram, M.K., Xu, X., Tan, B.Y., Venketasubramanian, N., Postma, A., Biessels, G.J., Chen, C.P., 2016. Impact of strategically located white matter hyperintensities on cognition in memory clinic patients with small vessel disease. PLoS One 11, e0166261.
Biesbroek, J.M., Weaver, N.A., Biessels, G.J., 2017. Lesion location and cognitive impact of cerebral small vessel disease. Clin. Sci. (Lond.) 131, 715–728.
de Groot, M., Ikram, M.A., Akoudad, S., Krestin, G.P., Hofman, A., van der Lugt, A., Niessen, W.J., Vernooij, M.W., 2015. Tract-specific white matter degeneration in aging: the Rotterdam study. Alzheimers Dement. 11, 321–330.
Desikan, R.S., Segonne, F., Fischl, B., Quinn, B.T., Dickerson, B.C., Blacker, D., Buckner, R.L., Dale, A.M., Maguire, R.P., Hyman, B.T., Albert, M.S., Killiany, R.J., 2006. An automated labeling system for subdividing the human cerebral cortex on MRI scans into gyral based regions of interest. NeuroImage 31, 968–980.
Diao, L., Yu, H., Zheng, J., Chen, Z., Huang, D., Yu, L., 2015. Abnormalities of the uncinate fasciculus correlate with executive dysfunction in patients with left temporal lobe epilepsy. Magn. Reson. Imaging 33, 544–550.
Duering, M., Zieren, N., Herve, D., Jouvent, E., Reyes, S., Peters, N., Pachai, C., Opherk, C., Chabriat, H., Dichgans, M., 2011. Strategic role of frontal white matter tracts in vascular cognitive impairment: a voxel-based lesion-symptom mapping study in CADASIL. Brain 134, 2366–2375.
Duering, M., Gonik, M., Malik, R., Zieren, N., Reyes, S., Jouvent, E., Herve, D., Gschwendtner, A., Opherk, C., Chabriat, H., Dichgans, M., 2013. Identification of a strategic brain network underlying processing speed deficits in vascular cognitive impairment. NeuroImage 66, 177–183.
Duering, M., Gesierich, B., Seiler, S., Pirpamer, L., Gonik, M., Hofer, E., Jouvent, E., Duchesnay, E., Chabriat, H., Ropele, S., Schmidt, R., Dichgans, M., 2014. Strategic white matter tracts for processing speed deficits in age-related small vessel disease. Neurology 82, 1946–1950.
Fischl, B., Salat, D.H., Busa, E., Albert, M., Dieterich, M., Haselgrove, C., van der Kouwe, A., Killiany, R., Kennedy, D., Klaveness, S., Montillo, A., Makris, N., Rosen, B., Dale, A.M., 2002. Whole brain segmentation: automated labeling of neuroanatomical structures in the human brain. Neuron 33, 341–355.
Hau, J., Sarubbo, S., Perchey, G., Crivello, F., Zago, L., Mellet, E., Jobard, G., Joliot, M., Mazoyer, B.M., Tzourio-Mazoyer, N., Petit, L., 2016. Cortical terminations of the inferior Fronto-occipital and Uncinate fasciculi: anatomical stem-based virtual dissection. Front. Neuroanat. 10, 58.
Hindmarch, I., Lehfeld, H., de Jongh, P., Erzigkeit, H., 1998. The Bayer activities of daily living scale (B-ABL). Dement. Geriatr. Cogn. Disord. 9, 20–26.
Hua, K., Zhang, J., Wakana, S., Jiang, H., Li, X., Reich, D.S., Calabresi, P.A., Pekar, J.J., van Zijl, P.C., Mori, S., 2008. Tract probability maps in stereotaxic spaces: analyses of white matter anatomy and tract-specific quantification. NeuroImage 39, 336–347.
Jiang, J., Sachdev, P., Lipnicki, D.M., Zhang, H., Liu, T., Zhu, W., Suo, C., Zhuang, L., Crawford, J., Reppermund, S., Trollor, J., Brodaty, H., Wen, W., 2014. A longitudinal study of brain atrophy over two years in community-dwelling older individuals. NeuroImage 86, 203–211.
Lovden, M., Kohncke, Y., Laukka, E.J., Kalpouzos, G., Salami, A., Li, T.Q., Fratiglioni, L., Backman, L., 2014. Changes in perceptual speed and white matter microstructure in the corticospinal tract are associated in very old age. NeuroImage 102, 520–530.
Madden, D.J., Bennett, I.J., Burzynska, A., Potter, G.G., Chen, N.K., Song, A.W., 2012. Diffusion tensor imaging of cerebral white matter integrity in cognitive aging. Biochim. Biophys. Acta 1822, 386–400.
Maniega, S.M., Valdes Hernandez, M.C., Clayden, J.D., Royle, N.A., Murray, C., Morris, Z., Aribisala, B.S., Gow, A.J., Starr, J.M., Bastin, M.E., Deary, I.J., Wardlaw, J.M., 2015. White matter hyperintensities and normal-appearing white matter integrity in the aging brain. Neurobiol. Aging 36, 909–918.
Mann, S.L., Hazlett, E.A., Byne, W., Hof, P.R., Buchsbaum, M.S., Cohen, B.H., Goldstein, K.E., Haznedar, M.M., Mitsis, E.M., Siever, L.J., Chu, K.W., 2011. Anterior and posterior cingulate cortex volume in healthy adults: effects of aging and gender differences. Brain Res. 1401, 18–29.
Metzler-Baddeley, C., Jones, D.K., Steventon, J., Westacott, L., Aggleton, J.P., O'Sullivan, M.J., 2012. Cingulum microstructure predicts cognitive control in older age and mild cognitive impairment. J. Neurosci. 32, 17612–17619.
Pantoni, L., 2010. Cerebral small vessel disease: from pathogenesis and clinical characteristics to therapeutic challenges. Lancet Neurol. 9, 689–701.
Park, D.C., Reuter-Lorenz, P., 2009. The adaptive brain: aging and neurocognitive scaffolding. Annu. Rev. Psychol. 60, 173–196.
Pekala, J.S., Mamourian, A.C., Wishart, H.A., Hickey, W.F., Raque, J.D., 2003. Focal lesion in the splenium of the corpus callosum on FLAIR MR images: a common finding with aging and after brain radiation therapy. AJNR Am. J. Neuroradiol. 24, 855–861.
Petersen, R.C., 2004. Mild cognitive impairment as a diagnostic entity. J. Intern. Med. 256, 183–194.
Prins, N.D., Scheltens, P., 2015. White matter hyperintensities, cognitive impairment and dementia: an update. Nat. Rev. Neurol. 11, 157–165.
Raji, C.A., Lopez, O.L., Kuller, L.H., Carmichael, O.T., Longstreth, W.T., Gach, H.M., Boardman, J., Bernick, C.B., Thompson, P.M., Becker, J.T., 2012. White matter lesions and brain gray matter volume in cognitively normal elders. Neurobiol. Aging 33.
Sachdev, P., 2005. Should we distinguish between periventricular and deep white matter hyperintensities? Stroke 36, 2342–2343.
Sachdev, P.S., Brodaty, H., Reppermund, S., Kochan, N.A., Trollor, J.N., Draper, B., Slavin, M.J., Crawford, J., Kang, K., Broe, G.A., Mather, K.A., Lux, O., Memory Ageing Study Team, 2010. The Sydney Memory and Ageing Study (MAS): methodology and baseline medical and neuropsychiatric characteristics of an elderly epidemiological non-demented cohort of Australians aged 70–90 years. Int. Psychogeriatr. 22, 1248–1264.
Smith, E.E., Salat, D.H., Jeng, J., McCreary, C.R., Fischl, B., Schmahmann, J.D., Dickerson, B.C., Viswanathan, A., Albert, M.S., Blacker, D., Greenberg, S.M., 2011. Correlations between MRI white matter lesion location and executive function and episodic memory. Neurology 76, 1492–1499.
Turken, A., Whitfield-Gabrieli, S., Bammer, R., Baldo, J.V., Dronkers, N.F., Gabrieli, J.D., 2008. Cognitive processing speed and the structure of white matter pathways: convergent evidence from normal variation and lesion studies. NeuroImage 42, 1032–1044.
van der Vlies, A.E., Staekenborg, S.S., Admiraal-Behloul, F., Prins, N.D., Barkhof, F., Vrenken, H., Reiber, J.H.C., Scheltens, P., van der Flier, W.M., 2013. Associations between magnetic resonance imaging measures and neuropsychological impairment in early and late onset Alzheimer's disease. Alzheimer Dis. 35, 169–178.
Wen, W., Sachdev, P.S., Chen, X.H., Anstey, K., 2006. Gray matter reduction is correlated with white matter hyperintensity volume: a voxel-based morphometric study in a large epidemiological sample. NeuroImage 29, 1031–1039.
Wen, W., Sachdev, P.S., Li, J.J., Chen, X., Anstey, K.J., 2009. White matter hyperintensities in the forties: their prevalence and topography in an epidemiological sample aged 44–48. Hum. Brain Mapp. 30, 1155–1167.
Winblad, B., Palmer, K., Kivipelto, M., Jelic, V., Fratiglioni, L., Wahlund, L.O., Nordberg, A., Backman, L., Albert, M., Almkvist, O., Arai, H., Basun, H., Blennow, K., de Leon, M., DeCarli, C., Erkinjuntti, T., Giacobini, E., Graff, C., Hardy, J., Jack, C., Jorm, A., Ritchie, K., van Duijn, C., Visser, P., Petersen, R.C., 2004. Mild cognitive impairment - beyond controversies, towards a consensus: report of the international working group on mild cognitive impairment. J. Intern. Med. 256, 240–246.
Wu, W.C., Poser, B.A., Douaud, G., Frost, R., In, M.H., Speck, O., Koopmans, P.J., Miller, K.L., 2016. High-resolution diffusion MRI at 7T using a three-dimensional multi-slab acquisition. NeuroImage 143, 1–14.